Available online at www.sciencedirect.com

jmr&t
Journal of Materials Research and Technology
www.jmrt.com.br

Original Article

The role of PVD sputtered PTFE and Al_2O_3 thin films in the development of damage tolerant coating systems

Chi-Ho Ng, Jeff Rao, John Nicholls*

Surface Engineering and Precision Institute (SEPi), School of Aerospace, Transport and Manufacturing, Cranfield University, Bedford MK43 0AL, UK

ARTICLE INFO

Article history:
Received 9 October 2019
Accepted 5 November 2019
Available online 9 December 2019

Keywords:
PVD
PTFE
Al_2O_3
Damage tolerant coating
Self-lubricating

ABSTRACT

The surfaces of artificial joints are susceptible to premature wear which reduces their service life leading to the increased risk of revision arthroplasty. Tribological coatings having low coefficients of friction (CoF) and which are also biocompatible are therefore required to minimise such risks.

Metal matrix composite (MMC) coatings exhibiting a modified toughness structure, thus reducing the potential to crack were successfully fabricated by cold spray (CS) technology. The coatings comprised of an ultra-low wear polytetrafluoroethylene (PTFE) + alumina (Al_2O_3) composite, firstly delineated by Burris and Sawyer in 2006, were prepared on cold sprayed substrate and the functionality of such coatings in terms of enhanced frictional properties was investigated.

In this study, PTFE + Al_2O_3 thin film coatings were prepared by physical vapour deposition (PVD) and incorporated with cold sprayed MMC coatings to produce a damage tolerant coating system designed to extend the service life of artificial movable joint surfaces.

Surface characterisation analysis indicated the formation of a PTFE–Al_2O_3 nanocomposite forming between the PTFE and Al_2O_3. This composite thin film exhibited excellent friction reducing ability up to an applied load of 7 N. Regardless of whether the Ti–6Al is manufactured by a layer-by-layer approach or co-sputtering method, the CoF is reduced to below 0.1 at the start of the test. Furthermore, the results reveal that the PVD sputtered PTFE + Al_2O_3 thin film functionalises the cold sprayed surface by offering a self-lubricating effect and that PVD combined with CS is reliable for devising material systems operating in high-wear applications.

© 2019 The Authors. Published by Elsevier B.V. This is an open access article under the CC BY-NC-ND license (http://creativecommons.org/licenses/by-nc-nd/4.0/).

1. Introduction

At present, existing artificial joints perform around 15 years of useful service life before failure because of the many factors affecting the long-term stability of contact parts in artificial joints, such as stress levels on contacting surfaces, material

* *Corresponding author.*
E-mail: J.Rao@cranfield.ac.uk (J. Rao).
https://doi.org/10.1016/j.jmrt.2019.11.009
2238-7854/© 2019 The Authors. Published by Elsevier B.V. This is an open access article under the CC BY-NC-ND license (http://creativecommons.org/licenses/by-nc-nd/4.0/).

properties and aseptic loosening [1]. The underlying reason for implant failure (aseptic loosening) is associated to the body's response to the wear debris generated from load-bearing surfaces, inducing osteolysis. Therefore, a convincible approach to improve the reliability and durability of artificial joints is targeted to engineer these surfaces with an impact resilience and damage tolerant coating.

In a previous study [2], Ti metal matrix composite (MMC) coatings were successfully manufactured by cold spray (CS) technology producing reliable bearing surfaces for artificial joints with the virtue of impact and damage tolerance. However, the frictional properties of these MMC coatings were demonstrated to be insufficient to diminish the wear damage of slider and counter surfaces. Therefore, these MMC coatings can only be an undercoat on the surface of the implant, providing protection against impact rather than wear. With regards to the improvement in tribological properties, this undercoat should be integrated with a wear resistant topcoat to form a coating system with the provision of impact, wear and damage protection for artificial implants. Under these circumstances, self-lubricating materials may be one of the realistic alternatives as a topcoat for governing friction and wear.

Polytetrafluoroethylene (PTFE) is a popular self-lubricating material because it is chemically inert and inherits a relatively lower CoF amongst polymeric materials. Its application in bearing and sealing is well known [3,4] as their low frictional properties are usually associated with simple shearing of weak interlayer bonds (bonded by van der Waals force). Moreover, PTFE has been widely used in biomedical and pharmaceutical applications due to its good mechanical properties and non-reactive functionality with organic substances [5]. For example, biliary metal stents incorporated with expanded PTFE (e-PTFE) were fabricated to controlled tumour ingrowth and it shows less tumour ingrowth when compared to polyurethane (PU) [6]. Moreover, e-PTFE has shown preferred mechanical characteristics in soft tissue engineering for its bio integrity [7]. The fluorinated polymers (e.g. PTFE) also has been proved to exhibit both a lower thrombogenicity and decreased inflammatory response [8]. Furthermore, fluorinated polymers can cause a decrease in platelet adhesion and activation, and improve a better blood compatibility [9]. The above evidence indicated that PTFE has good compatibility with human body, which is commonly employed in biomedical applications. However, PTFE cannot be applied as a self-lubricating topcoat alone due to its inferior mechanical strength and abrasion resistance as has been demonstrated [10,11].

Composite coatings containing PTFE have been considered over the past decade because of their improved wear protection in terms of lubricity and rubbing mechanisms. For example, PTFE co-deposited with antimicrobial metal (e.g. Ag) to achieve a self-lubricating effect [12], the result showed that a large majority of the electrodeposited coatings still adhered to the substrate with improved wear performance. Higher hardness metal oxide particles with good biocompatibility, such as Al_2O_3 and TiO_2 have been investigated with the incorporation of PTFE to improve the wear resistance of coatings [13,14]. Composite coatings with a particular focus on the incorporation of PTFE and metal oxide particles may be an alternative to facilitate the CS MMC undercoat with a high micro-hardness and good self-lubricating property as well as the protection for the opposing surface. Sawyer et al. demonstrated a 600× improvement in wear resistant of PTFE–Al_2O_3 nanocomposite and their wear resistant enhanced monotonically with increasing filler concentration [15]. Furthermore, Burris and Sawyer continued the investigation of the optimum addition of nanoparticles, concluding that 5 w.t.% Al_2O_3 particles addition resulted in producing the lowest steady wear rate and steady CoF compared to unfilled PTFE [16]. The relatively low friction and superior wear resistant of these composites are in conjunction with the formation of a thin, robust and adherent polymeric tribofilm on both sliding surface [15–17]. Moreover, the wear debris generated from the composite coatings can serve as a third-body lubricant which is beneficial in the overall tribological performance, better protecting the CS MMC undercoat by this composite coating rather than a typical hard coating because the wear debris can become entrapped and act as a source of abrasive particles within the wear mechanism.

Physical vapour deposition (PVD) is an effective deposition method to fabricate a uniform thin film at a low working temperature [18,19]. However, to the best of our knowledge, the investigation on the functionalisation of PVD sputtered PTFE–Al_2O_3 composite film on CS MMC undercoat have rarely been reported. The main concept of this study is to functionalise the CS MMC undercoat by the PVD sputtered PTFE–Al_2O_3 composite film in order to improve the wear resistant and frictional properties. This research continues our previous study [2] to increase the flexibility of combining desirable characteristics of the materials, which can be one of the first attempts to improve the durability of artificial joint implants. In addition, a new concept of a damage tolerant coating system (PTFE + Al_2O_3 + MMC composite) applied on biomedical applications has been introduced by the implementation of two different low-cost coating technologies (PVD + CS).

2. Experimental details

2.1. *PVD magnetron sputtering*

Three different composition of metal matrix composite (MMC) coatings were produced by cold spray (CS) technology (using an in-house cold spray system in Trinity College Dublin, Ireland), namely, 94 w.t.% Grade 5 Ti + 6 w.t.% Al (refer to "Ti–6Al"), 90 w.t.% Grade 5 Ti + 10 w.t.% Al (refer to "Ti–10Al") and 50 w.t.% Grade 5 Ti + 50 w.t.% Al (refer to "Ti–50Al"). The experimental procedures and parameters followed the previous study [2].

Prior to PVD magnetron sputtering, the cold sprayed surface was polished using a series of grit-lined paper starting with 120-grit and finishing with 2500-grit paper to ensure surface homogeneity. A similar amount of time (i.e. around 10–15 mins per step), same speed (i.e. 150 rpm) and same applied force (i.e. 25 N) were used on each sample until the surface was flat and there were no obvious macro-pores. Struers Tegrapol-31 Grinder Polisher was used for this purpose. The PTFE and Al_2O_3 coatings were fabricated at room temperature using a Leybold L560® coater (two 3-inch magnetrons were equipped in the machine). The system was turbo-pumped to a base pressure to approximately 1×10^{-6} mbar before starting deposition. Argon was used as working gas due to its inertness

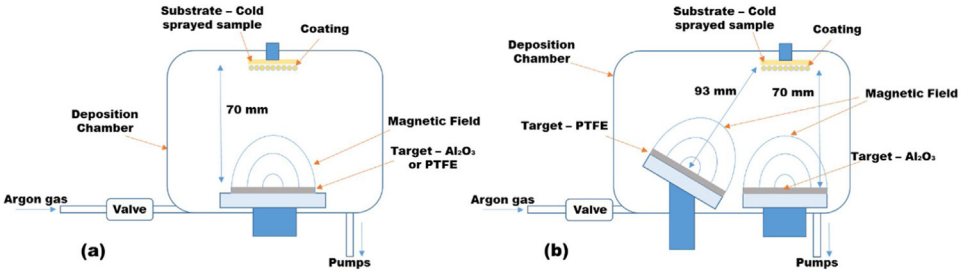

Fig. 1 – Schematic illustration of PVD magnetron sputtering: (a) layer-by-layer approach and (b) co-sputtering approach.

and a baratron was used to control the experimental process pressures. The target-to-substrate distance was constant at 70 mm to fix the power density used and the targets were sputter-cleaned (pre-sputtering) to remove any contamination for 5 min prior to sputtering.

The thin film coating was fabricated by placing the cold-sprayed substrate above the first magnetron and sputtering for a predetermined time. Afterwards, the substrate was moved to the second magnetron and the second material sputtered for a predetermined time, thus fabricating a thin film coating by the conventional layer-by-layer approach [20]. Firstly, Al_2O_3 was coated using ENI® pulsed DC power (f = 250 kHz, rate 1.056 μs) supply operating at 250 W at an argon gas pressure of 0.01 bar. Afterwards, PTFE was deposited onto Al_2O_3 coated samples using a radio frequency (13.56 MHz) power supply at 100 W at an argon gas pressure of 0.025 bar. Both sputtering processes were pre-determined to sputter for 300 min. Cold spray samples deposited by PVD sputtering (layer-by-layer approach) are referred to as "PVD Ti–6Al", "PVD Ti–10Al" and "PVD Ti–50Al".

The co-sputtering route was also implemented in order to examine the self-lubricating effect of co-sputtered PTFE and Al_2O_3 thin film coatings, and also enable a comparison in the frictional characteristics between the layered coating to be made. For the co-sputtering process, the MMC coating substrate was placed above the Al_2O_3 target and the sputtering deposition was done by operating both targets simultaneously. The target-to-substrate distance was kept at 70 mm for Al_2O_3 targets to fix the power density used, however, the PTFE target is angled to around 20° with respect to the vertical, with a target-to-substrate distance at 93 mm for sputtering. An argon gas pressure of 0.015 bar was used in the co-sputtering deposition. The schematic illustration of PVD magnetron sputtering for layer-by-layer approach and co-sputtering approach is shown in Fig. 1. Cold spray samples deposited by PVD co-sputtering are referred to as "CPVD Ti–6Al", "CPVD Ti–10Al" and "CPVD Ti–50Al" accordingly.

2.2. *PVD thin film coatings characterisation*

The cross-sectional images of the PVD sputtered PTFE + Al_2O_3 coatings were observed using a SEM equipped with energy dispersive X-ray spectroscopy (EDX, Oxford Instruments) and a focused ion beam (FIB) equipment (Tescan Lyra3). The FIB instrument was equipped with a dual beam plus SEM inside a vacuum chamber. The dual beam was used to firstly sputter-etch the sample which was then placed under the SEM. A thin platinum layer was coated on the sample surface for the protection of the coating. This platinum coated sample was sputtered by a finely focused gallium ions (Ga+) beam operated using a small current. A high current milling operation was subsequently applied to make a cross-sectional image of the PVD coated samples.

The surface roughness (R_a) of PVD sputtered samples was determined by stylus surface profilometry (Veeco Dektak3 ST). The results were calculated from the average of ten data with the standard deviation for the comparison between before and after PVD magnetron sputtering. Scratch testing (Teer Scratch Tester) was performed using a Rockwell diamond ball indenter (200 μm diameter) under continuous progressive loads with forces increasing from 5 N to 60 N, loading rate of 30 N/min and linear velocity of 6 mm/min with maximum friction force of 100 N. Furthermore, the Rockwell indentation was performed by Teer Scratch Tester and the applied loads were predefined as 10 N, 20 N, 30 N and 40 N which was to determine the corresponding stress in certain areas within the scratch track.

3. Results and discussion

3.1. *Surface roughness and coating analysis*

The CS samples were polished prior to coating using a series of grit-loaded papers up to 2500-grit to achieve a homogeneous surface and reduce the surface variability. The measured thickness after surface grinding with 120-grit paper decreased significantly (shown in Table 1 and Fig. 2). For Ti–50Al, the thickness reduced by 43%, compared with 62% and 52%, for the Ti–6Al and Ti–10Al samples, respectively.

A relatively insignificant change in surface roughness was measured after PVD magnetron sputtering of PTFE and Al_2O_3. There were slight differences between the three different samples. In Table 2, the surface roughness of thin film depends on the surface morphology of the substrate, typical of a PVD deposited film. Furthermore, the PVD process produces coatings at a relatively lower deposition temperature than other deposition processes (e.g. CVD) [21], reducing the formation of large clusters thereby producing a smoother surface.

It is interesting to note that the surface roughness of Ti–50Al was slightly higher than Ti–6Al or Ti–10Al after the same polishing procedure. The underlying reason can be explained by the different hardness and density of Grade 5 Ti and Al. For the Ti–50Al, considering there is more Al content in the material structure and Al has a faster material removal rate than Grade 5 Ti (i.e. Al is softer than Grade 5 Ti), a randomly

Table 1 – Coating thickness of cold sprayed samples before and after polished.

	Ti–6Al	Ti–10Al	Ti–50Al
Before polishing (μm)	1014.4 ± 59.0	952.0 ± 37.9	1197.4 ± 27.3
After polishing (μm)	384.4 ± 4.0	457.6 ± 2.1	677.0 ± 5.8

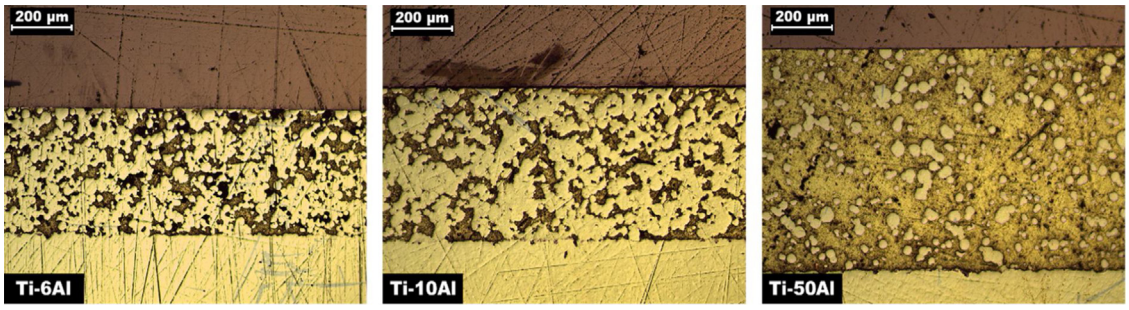

Fig. 2 – Cross-section images of cold sprayed samples after polishing.

Table 2 – Surface roughness (R_a, μm) of polished cold sprayed samples and PVD sputter (PTFE + Al_2O_3) samples.

	Ti–6Al	Ti–10Al	Ti–50Al
Before PVD sputtering (R_a, μm)	0.25 ± 0.07	0.24 ± 0.03	0.29 ± 0.03
After PVD sputtering (R_a, μm)	0.22 ± 0.04	0.29 ± 0.08	0.30 ± 0.05

distributed of Grade 5 Ti and Al particle on the sample surface can cause an imbalance of material removal and irregular surface finishing after polishing. Furthermore, notches and porosity in the CS sample may probably increase the difficulty of the polishing process to achieve the desired surface smoothness. Therefore, the polished Ti–50Al are rougher compared with the other samples despite the same polishing protocol being employed. The measured roughness of Ti–50Al is within the measurement error range of the current study, so it is assumed that the deposition of PTFE and Al_2O_3 films on Ti–50Al does not change much compared with other samples.

Fig. 3 shows the SEM cross-section image of a PVD sputtered (PTFE + Al_2O_3) CS sample, which in the first instance the image emerges as distinct layers across the top surface of the sample. By filtering only $K\alpha^1$ X-rays from C, F, Al and O via line scan EDX analysis, three distinct material zones can be clearly identified. The molecular structure of PTFE consists of a long chain of carbon atoms, similar to other polymers such as, polyethene, polypropene and polychloroethene (PVC). However, the PTFE chain is uniquely surrounded by fluorine atoms with strong bonding between carbon and fluorine atoms, which shields the vulnerable carbon chain. The presence of fluorine in the EDX line scan result implies that the PTFE thin film was intentionally deposited as the top layer. Moreover, the intensity ratio between carbon and fluorine content was approximately to 1:2 (i.e. each carbon atom attaches to two fluorine atoms in PTFE) and almost only carbon and fluorine were detected, further supporting the presence of PTFE above the Al_2O_3 thin film. From the top PTFE layer, according to the signal obtained by EDX, the C and F signal gradually decrease towards the cold sprayed subsurface. Meanwhile, the Al and O signals increase from zero to the peak value of ~190 and ~120, respectively. The aluminium-rich and oxygen-rich signals were detected in the region between the PTFE zone and the cold-sprayed subsurface, which is a good demonstration of the favourable deposition of Al_2O_3 prior to the deposition of the PTFE film [22].

The sample was tilted to 52° in the SEM for image capture, revealing that the PTFE + Al_2O_3 self-lubricating coating was approximately 2.25 μm thick, slightly lower than the sum of the PTFE and Al_2O_3 coatings which have a thickness of about 1.72 μm and 0.69 μm, respectively. A significant amount of fluorine was detected in the area between the PTFE zone and cold sprayed subsurface, indicating a certain level of hybridization between PTFE and Al_2O_3, forming a PTFE–Al_2O_3 mixed zone or creating PTFE–Al_2O_3 nanocomposite. The feasibility of hybridization is believed to be the interaction between the electronegative fluorine in PTFE and the positive charge of the Al cation in Al_2O_3. A similar observation was also reported in a previous study [19]. A continuous layer of PTFE extends parallel to the substrate, depositing additional PTFE along the columnar boundaries to create a nanocomposite or PTFE mixed zone. To further confirm this hypothesis, TEM images of the self-lubricating layer should be taken to support the EDX findings which suggest some degree of hybridization between PTFE and Al_2O_3.

The deposition rate is one of the key factors affecting the volume fraction of each material deposited on the cold sprayed subsurface influencing the structure and properties of the PVD sputtered thin film. The deposition rates of PTFE and Al_2O_3 were calculated to be 5.7 nm/min and 2.3 nm/min, respectively. Reported from the literature, the deposition rate of PTFE ranges between 20 nm/min and 90 nm/min [23–25], and the deposition rate of Al_2O_3 is in the range of 21–67 nm/min [26], 1–4 nm/min [27] and 11.6–30 nm/min [28]. The deposition rate of PTFE demonstrates a relatively lower value than the obtained by other studies. The inconsistent result indicates that the PVD magnetron sputtering is highly dependent on

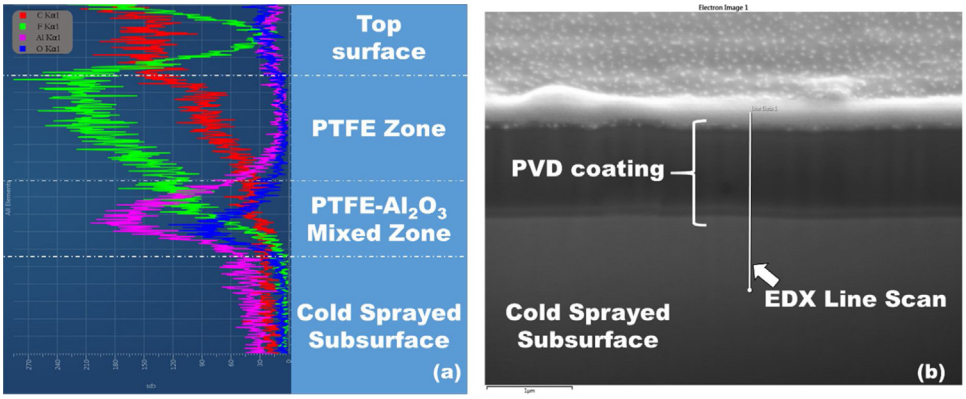

Fig. 3 – (a) The line scan EDS results and (b) the cross-section SEM image of PVD magnetron sputtered Ti–6Al cold sprayed sample.

the magnetic strength and the process conditions of the magnetron. The magnetic flux strength efficiency is not usually considered nor measured as long as supporting occurs, but this could be partially responsible for discrepancies between measured deposition rates by different studies, in addition to process conditions such as operating temperature or deposition pressure which are well documented to have a strong impact on deposition efficiency, chemical composition and microstructure of the PVD sputtered thin film.

Compared to reactive DC sputtering and RF sputtering, the deposition rate of pulsed DC sputtering is generally greater [29]. Therefore, due to the different power supplies used, DC versus RF, it should be assumed that deposition rate of Al_2O_3 (i.e. DC sputtering) is greater than that of PTFE (i.e. RF sputtering). However, the findings in this study demonstrate the opposite phenomenon. The reasons may be attributed to dissimilarities in material properties (i.e. polymer and ceramic), differences in magnetic flux strength efficiencies and different processing parameters (e.g. argon gas flow and pressure) used for PTFE and Al_2O_3 deposition. A continuous Al_2O_3 layer can still be deposited between the PTFE layer and the cold sprayed subsurface, albeit the deposition rate is relatively low. PTFE, with a relatively high deposition rate, results in functionalising the thin Al_2O_3 layer to create a nanocomposite structure by the layer-by-layer approach. The synergistic effect will be amplified to increase the wear resistance and decrease the CoF during sliding by combining the merit of self-lubricating polymer and high-hardness ceramic.

3.2. *Scratch test coating performance of layered PVD films*

The CS samples with and without a PVD sputtered (PTFE + Al_2O_3) thin film are evaluated by conducting a scratch test the results of which are shown in Figs. 4 and 5. The coefficient of friction (CoF) of the surfaces was recorded with the respective critical forces being applied by the stylus. The variation in CoF of the coating illustrates its performance and the different wear mechanisms of the cold-sprayed substrates and the PVD sputtered surface. The difference in CoF performance (as shown in Fig. 4) may be due to the generation of wear debris, which becomes entrapped between the stylus and sample surface increasing the wear rate. The increased CoF has also probably arisen from the increase of applied load and the real contact area between the coating surface and stylus, with the energy loss caused by plastic deformation of the wear debris and contact surface. Without a coating, the cold-sprayed samples exhibit a relatively higher CoF than the samples with a coating, with no major difference in the CoF between Ti–6Al and Ti–10Al (shown in Fig. 4). With a sputtered coating deposited on the cold-sprayed surface, not only did the CoF over the entire scratch distance reduce considerably, but the PVD sputtered Ti–6Al also demonstrated the lowest CoF and best scratch performance to a load of approximately 20 N. The current result was in good agreement with previous studies of similar composite materials having superior frictional characteristics and wear resistance under similar tribological testing [30–33].

The self-lubricated thin film (PVD sputtered PTFE + Al_2O_3) on a cold-sprayed surface exhibits a lower CoF in the beginning of the test (especially for PVD sputtered Ti–6Al sample), and the CoF increased continuously with increasing load. For PVD sputtered Ti–50Al (as shown in Fig. 5), the CoF increased rapidly and it exhibited large wear debris generation and a wider wear track over the entire distance. Because of the low hardness of Ti–50Al [2], the load-bearing capacity of the damage tolerant coating system (PTFE + Al_2O_3 + Ti–50Al) is limited, exhibiting severe wear which is evidenced by the poor appearance on its surface. A higher overall CoF and almost non-existent self-lubricating regime were also presented for the PVD sputtered Ti–50Al, whereas, PVD sputtered Ti–6Al and Ti–10Al demonstrated a long-lasting self-lubricating effect with a steady growth and lower CoF.

Furthermore, as shown in Fig. 5, the scratch test profiles of the CoF could be split into four different regions. The first region defines as the onset of cohesive failure (the region on the left of the line labelled L1) and here the Ti–10Al sample transforms from a mixed to a boundary lubrication regime (CoF > 0.1), whereas the Ti–6Al transitions between a mixed and hydrodynamic lubrication regime, as shown in Zone 1. The most prominent self-lubricating effect occurs in the PVD sputtered Ti–6Al. This phenomenon can be further explained by Bowden and Tabor model of friction [34]. The friction coefficient can be expressed as $\mu = A^* S_m/W$, where A is the real

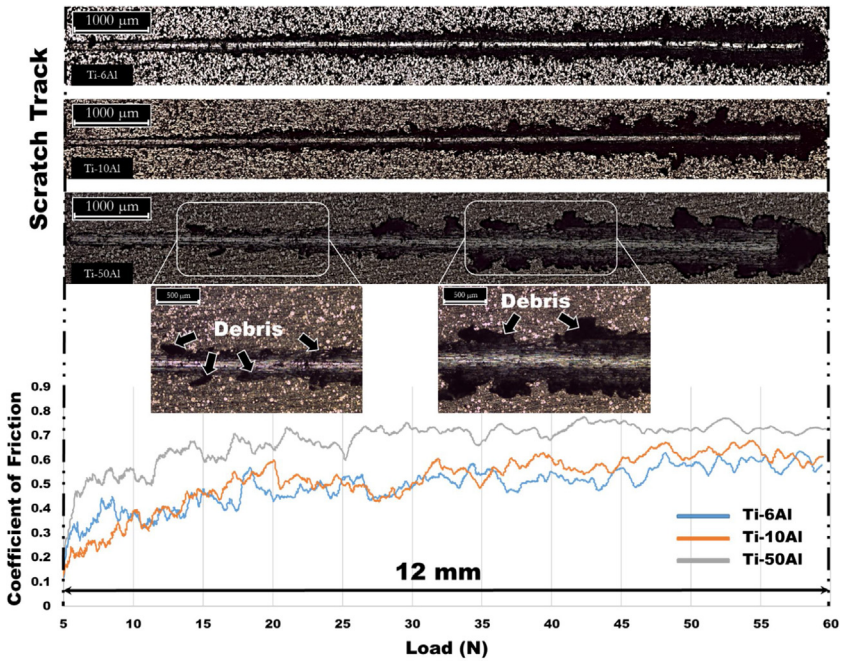

Fig. 4 – Optical scratch images of cold sprayed samples under linearly progressive load and the plot of coefficient of friction (CoF) against continuous progressive loads [2].

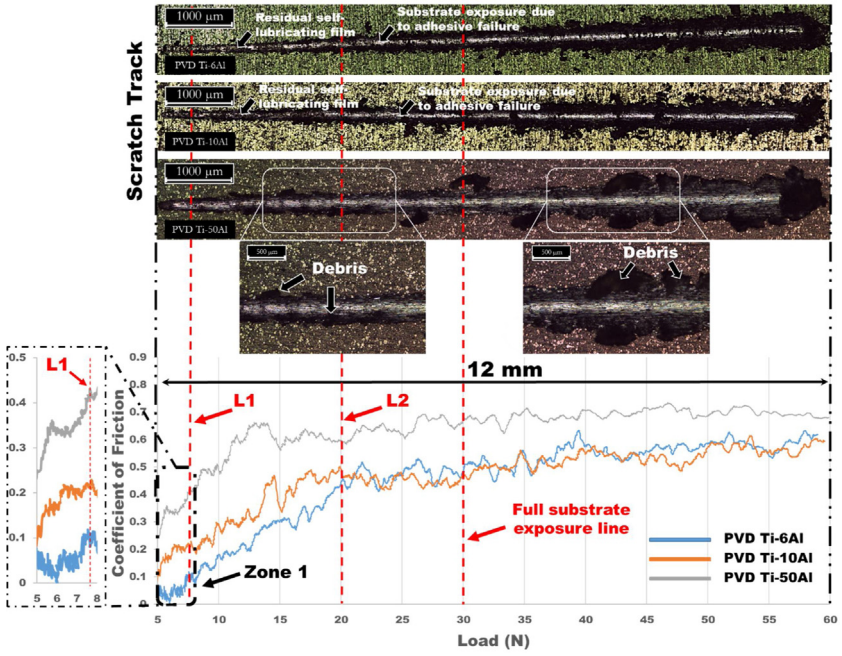

Fig. 5 – Optical image of linearly progressive load scratch on the cold sprayed samples with PVD sputtered (PTFE + Al_2O_3) thin film and the plot of coefficient of friction (CoF) against continuous progressive loads.

contact area, S_m is the constant mean shear stress and W is the normal load. Here, the real contact area between the PTFE + Al_2O_3 thin film and stylus increases with applied load, but the rate of applied load is greater than the real contact area, thus decreasing CoF along with increasing applied load. This in turn proves that the self-lubricating film and its wear debris (which acts as a solid lubricant) can provide sufficient lubrication during the sliding process, albeit the extent of this lubricious state is relatively short.

For the second region labelled between the lines L1 and L2, is defined as the zone between where cohesive to adhesive failure occurs in the coatings, and is the running-in period up to an applied load of 20 N, after which the CoF stabilizes. The CoF of Ti–6Al and Ti–10Al gradually increases from a CoF

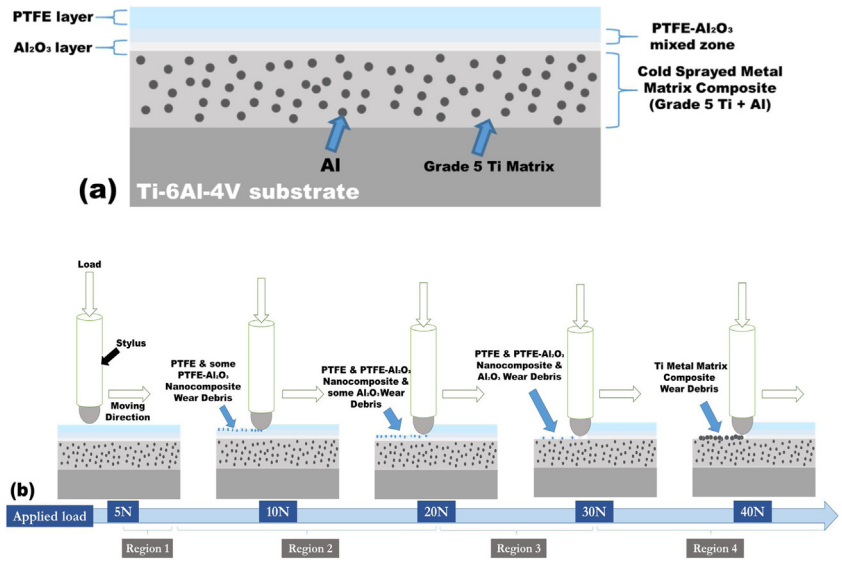

Fig. 6 – Schematic diagram of (a) the cross-sectional view of PVD magnetron sputtered Ti–6Al and (b) the evolution of wear behaviour of PVD magnetron sputtered Ti–6Al, indicating 4 different regions corresponding to CoF in Fig. 5.

around 0.1 to around 0.5 at a load of 60 N, whereas the Ti–50Al sample shows an initial steep rise in CoF up to a load of 15 N after which the CoF averages around 0.7 for loads up to 60 N. This suggests that the PTFE top layer in this sample is removed relatively easily and the PTFE–Al_2O_3 nanocomposite layer has already failed before an applied load of 15 N. The Al_2O_3 layer is a hard-ceramic coating without self-lubricating properties compared to PTFE and a PTFE–Al_2O_3 nanocomposite. Under similar loading conditions, an alumina coating would have greater measured CoF when it directly contacts the stylus. This is because the hard asperities of the Al_2O_3 surface are not easily deformed and the local pressures at these contact points are relatively higher than other coating layers, thus producing the higher CoF measured. Moreover, the boundary lubrication regime dominates the lubrication mechanism of PVD sputtered Ti–6Al and Ti–10Al within the second region (between the lines labelled L1 and L2), however, the damage of the self-lubricating film is greater with increasing applied loads, which reduces the load-bearing capacity of the coating and thus resulting in a shorter service life.

The adhesive failure of the coating can be observed in the third region, after 20 N, evidenced by the loss of the coating and the exposure of the substrate (region between L2 line and full substrate exposure line). Also, for this sample the CoF is comparatively higher than in the previous regions, but remains around 0.7 over this zone. The self-lubricating film (PTFE + Al_2O_3) is almost destroyed due to the loss of residual film and increase of substrate exposure, whereas, the residual wear debris continually acts as a solid lubricant inside the wear track and alleviates the increase in CoF.

The last region (region after full substrate exposure line) is the zone where the substrate is exposed, manifesting as having a wider and deeper wear track with high overall CoF and relatively large amplitude peaks (i.e. PVD Ti–6Al and PVD Ti–10Al) due to a larger contact area in front of the stylus. After 30 N, a slight increase in the CoF is perceived for all PVD coated samples and the remnant self-lubricating wear debris was no longer existence as a solid lubricant to mitigate the CoF. Subsequently, a new asperity boundary is formed on the delaminated surface by the stylus to accommodate the sliding process. The rising CoF is the response of the adhesive failure besides the wear track, which takes place when the inter-particle cracks reach a critical crack length causing a delamination of the cold sprayed subsurface. Four regions are well identified but critical loads lines are mainly assigned according to the performance of PVD sputtered Ti–6Al. The schematic diagram (Fig. 6) also assists to illustrate the cross-section view of the micro-structure of PVD sputtered Ti–6Al and its evolution of wear behaviour with respect to different applied loads.

The remarkable self-lubricating effect of PVD sputtered samples and the four identified regions can be further verified by the worn surface morphologies as shown in Fig. 7. Since the thin film (PTFE + Al_2O_3) provides superior surface protection along with self-lubricating properties on the cold sprayed Ti–6Al surface, less wear debris of small size is observed in the wear track of Ti–6Al signifying that this coating serves to reduce wear. The thin film surface is well preserved and adhered to the Ti–6Al surface as shown in region 1, which further supports the evidence of hydrodynamic lubrication within this region offering the best self-lubricating behaviour associated to the measured CoF shown in Fig. 5. The self-lubricating film on Ti–10Al surface suffers a certain level of damage in region 1, but still provides a limited self-lubricating effect and some degree in reducing the CoF. The contrasting behaviour of Ti–50Al in region 1 is apparent in Fig. 7, which shows the removal of the coating and a wider wear track can be observed. The residual wear debris no longer acts as a solid lubricant and offers the lowest level of CoF reduction as the substrate is clearly exposed.

As the loading regime continues to region 2, above loads of 10 N, there are increasing signs of adhesive failure with

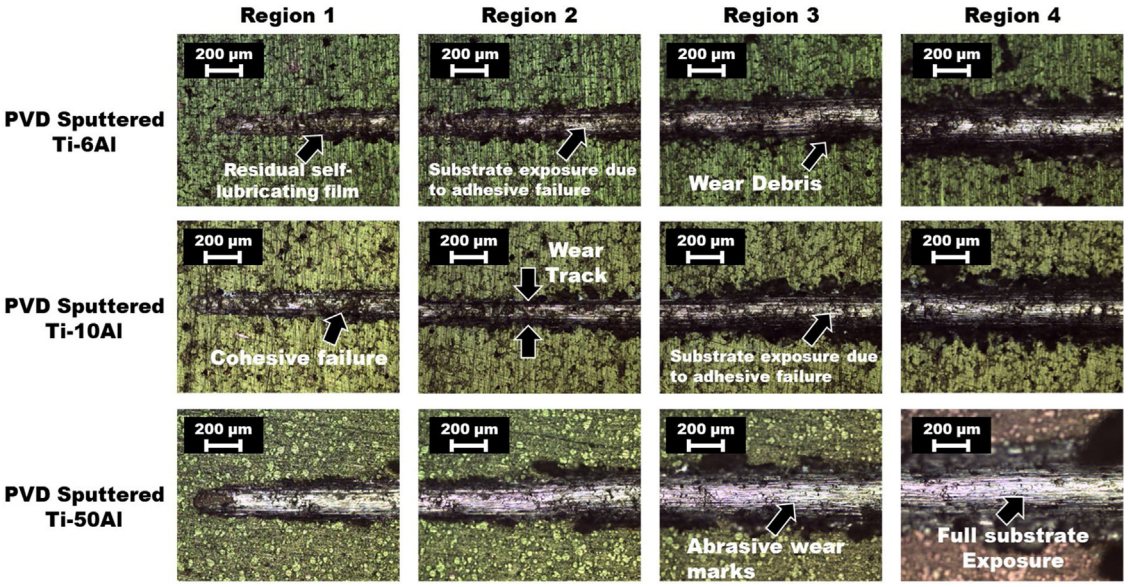

Fig. 7 – Worn surface morphologies of PVD sputtered samples on four different regions.

increasing load for the Ti–6Al and Ti–10Al samples. Furthermore, the wear mechanism of Ti–6Al and Ti–10Al progressively changes from adhesive to abrasive wear due to the complete removal of the self-lubricating thin film from the wear track. Evidence of abrasive wear manifests as relatively larger wear debris observed in regions 3 and 4 when the applied load exceeds 20 N, abrasive wear being the primary wear mechanism for PVD sputtered Ti–6Al and Ti–10Al. The inter-particle cracks on the worn surface in region 4 are also detected, representing delamination and cohesion bond failure of the cold-sprayed subsurface under high loads and the applied shear forces leading to increased CoFs and higher wear rates.

In region 1, comparing to the wear morphologies of Ti–6Al and Ti–10Al, the wear track of Ti–50Al exhibits severe abrasive wear. Moreover, Ti–50Al shows an evidence that when the load is in region 2, a lot of wear debris is generated. Entrapment of the self-lubricating wear debris from the PTFE and PTFE–Al_2O_3 nanocomposite could be responsible for the measured low CoF in this sample in region 1, but does not extend to region 2 where this self-lubricating layer is totally removed and no longer provides a tribo-film surface on the cold-sprayed Ti–50Al subsurface. Additionally, the abrasive wear marks on the worn surface become more apparent in regions 2–4 due to increasing applied loads. As evidenced by the width of the wear track, it is reasonable to assume that the coating system of PVD sputtered Ti–50Al possesses the lowest hardness and minimal self-lubricating effect, and it is primarily subject to abrasive wear when the applied load exceeds 10 N.

3.3. *Coating performance of co-sputtered PVD film in scratch test*

In PVD co-sputtering deposition, the PTFE target was placed further away from the substrate (the target-to-substrate distance was changed from 70 mm to 93 mm) and inclined to 20° with respect to the vertical. The relationship between the deposition rate and the target-to-substrate distance is deposition rate $\propto$ (1/(target-to-substrate distance)^2). The greater the distance from the target to substrate, the lower the PTFE deposition rate. Therefore, it is assumed that the PTFE–Al_2O_3 nanocomposite thin film prepared by the co-sputtering method is thinner than the thin film prepared by the layer-by-layer approach. Thus, it is proposed that the extent of the self-lubricating effect will be diminished and the wear protection for cold sprayed subsurface will be also minimised compared to the coatings produced by the layer-by-layer approach.

As per the layered coatings, the wear track can be divided into four regions as shown in Fig. 8, with regions 2 and 3 being significantly reduced for the co-sputtered coatings. The self-lubricating effect of the co-sputtering thin film is still most effective for the cold sprayed Ti–6Al, whether it is layered or co-sputtered Ti–6Al, they both exhibit similar friction behaviour in the range between mixed and the hydrodynamic lubrication region (shown in Zone 1). Most importantly, the co-sputtered PTFE–Al_2O_3 nanocomposite thin film can further reduce the CoF for cold sprayed Ti–10Al in region 1, showing characteristics of mixed and hydrodynamic lubrication regime albeit for a very short duration. Having a thinner self-lubricating thin film and without any PTFE topcoat, all co-sputtered samples progressively increase steeply from the L1 line. This initial large gradient in CoF may be associated with an increased contact of more cold sprayed subsurface and the stylus because of the complete removal of the nanocomposite film. The anti-friction effect provided by a self-lubricating thin film, either in layer-by-layer approach or co-sputtering route is insignificant on the surface of cold sprayed Ti–50Al. The anti-friction protection can only extend to an applied load of approximately 13 N in the case of a co-sputtered film. After 13 N, the friction behaviour fully represents the cold sprayed Ti–50Al subsurface and there is no any residual self-lubricating debris that remains in the wear track. It is intriguing that to note that the sudden drop in CoF as indicated by Zone 2, appears in region 3 (region between L2 line and full substrate exposure line), and could indicate

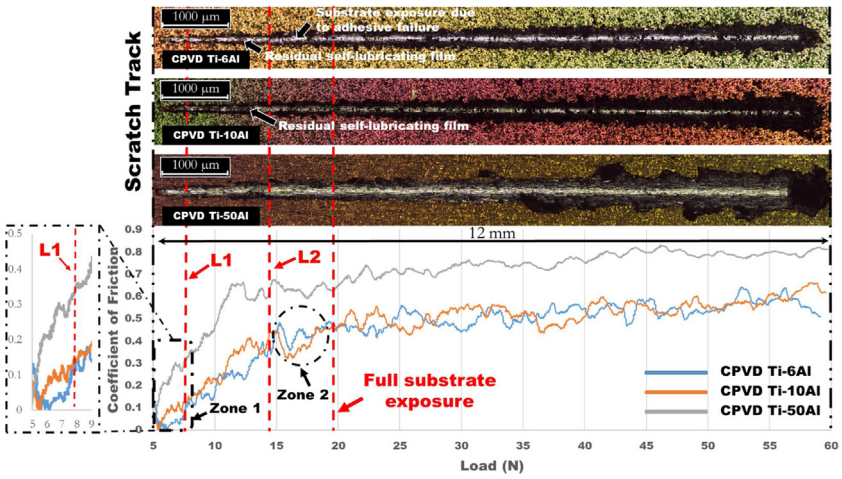

Fig. 8 – Optical image of linearly progressive load scratch on the cold sprayed samples with PVD co-sputtered (PTFE + Al_2O_3) thin film and the plot of coefficient of friction (CoF) against normal load.

remnant self-lubricating nano-composite debris which has accumulated in front of the wear track and the stylus before it is totally removed and the substrate exposed.

The surface morphologies of PVD co-sputtered samples are shown in Fig. 9. It was observed that the self-lubricating film was severely affected in region 1, even for the samples of co-sputtered Ti–6Al and Ti–10Al. This implies that the co-sputtered film has a relatively low bond strength and is removed by the relatively low applied loads of 6 N. According to the worn surface appearance in region 1 (as shown in Fig. 9) and CoF of PVD coated surface in Fig. 8, the reduced CoF is primarily due to the residual self-lubricating debris rather than the self-lubricating film which remains. The debris becomes entrapped between the stylus and the surface offering some degree of self-lubrication, this self-lubricating debris can prolong the protection from region 1 to region 3 (as shown in Fig. 8) but is completely removed with increasing loads, exposing the substrate, especially for the cases of co-sputtered Ti–6Al and Ti–10Al. For co-sputtered Ti–50Al, the early damage to the self-lubricating film in region 1 reduces the anti-friction effect from the self-lubricating debris and minimises the protection duration from the co-sputtered nanocomposite, which indicates inferior friction behaviour from the co-sputtered route rather than the layer-by-layer approach. The worn surface morphologies of regions 3 and 4 shown in Fig. 9 are similar to that observed in Fig. 7, they all suffered from abrasive wear under high applied loads and scratch motion, and had little or no anti-friction protection from self-lubricating debris on the exposed cold sprayed subsurface.

If certain conditions are taken into consideration, such as coating thickness, surface finishing and avoidance of cracks [35], it is possible to apply micro-indentation technique in the determination of adhesive/cohesive bond strength. Also, the applied indentation load should be lower than the value

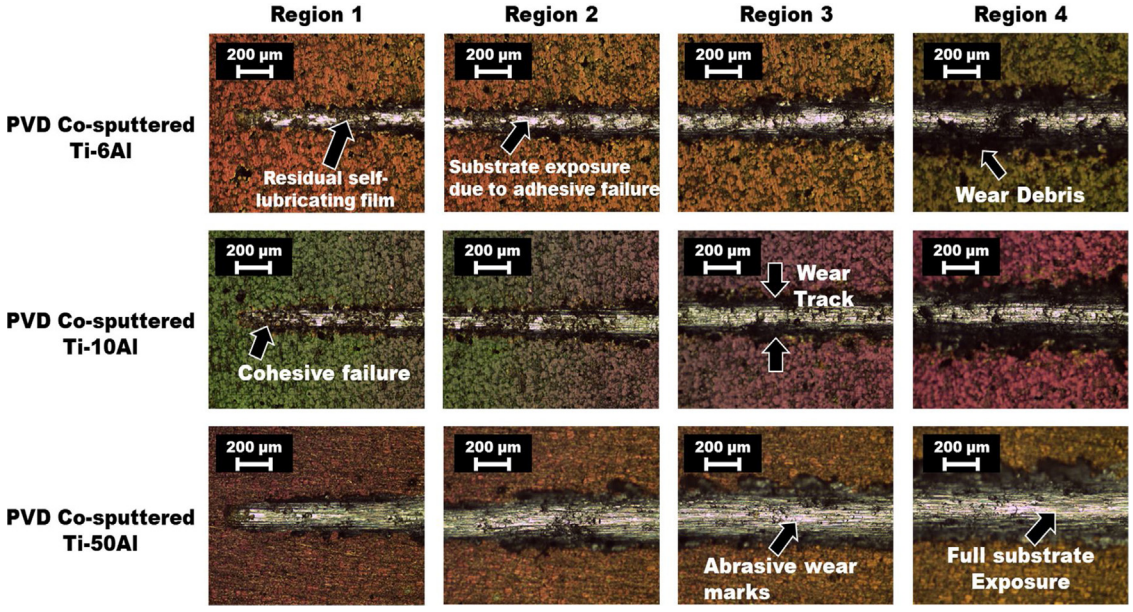

Fig. 9 – Worn surface morphologies of PVD Co-sputtered samples on four different regions.

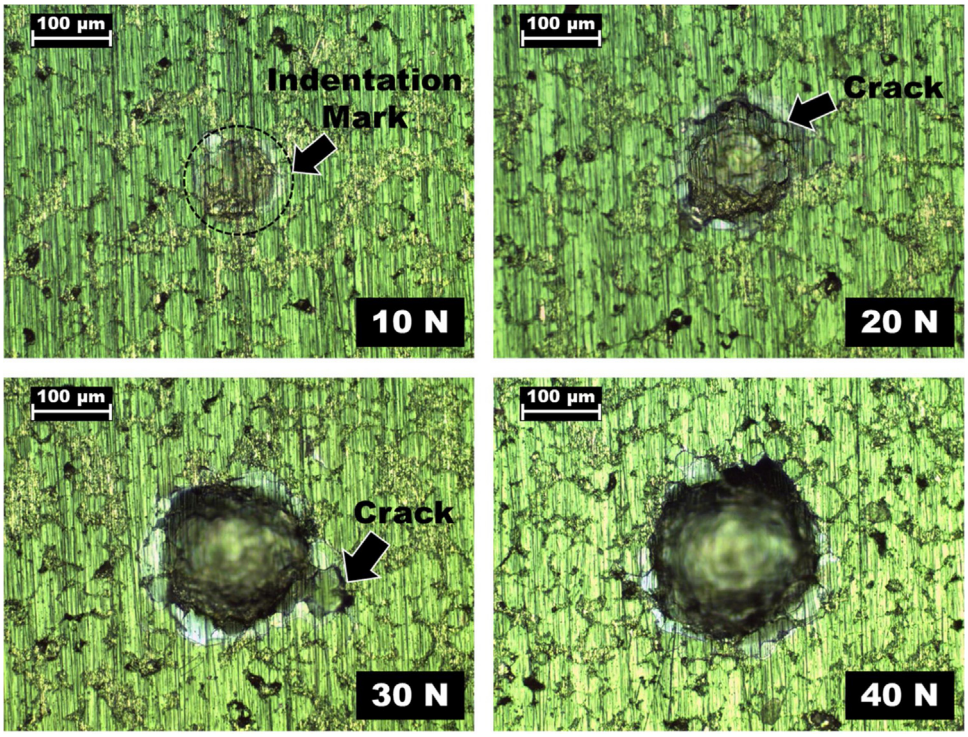

Fig. 10 – The optical images show the Rockwell indentation mark on PVD magnetron sputtered Ti–6Al sample with loads of 10 N, 20 N, 30 N and 40 N, respectively.

Table 3 – The corresponding coefficient of friction (CoF) with respect to critical load applied in scratch test for all samples with and without PVD sputtering.

Critical load (N)	Coefficient of friction (CoF)								
	Ti–6Al	Ti–10Al	Ti–50Al	PVD Ti–6Al	PVD Ti–10Al	PVD Ti–50Al	CPVD Ti–6Al	CPVD Ti–10Al	CPVD Ti–50Al
10	0.39	0.39	0.55	0.18	0.28	0.48	0.18	0.23	0.47
20	0.43	0.6	0.64	0.46	0.46	0.6	0.46	0.46	0.64
30	0.49	0.51	0.73	0.49	0.47	0.68	0.44	0.55	0.75
40	0.55	0.59	0.71	0.57	0.56	0.7	0.53	0.51	0.75

that create cracks on imprints, therefore, the obtained values of hardness and corresponding modulus of elasticity can be considered as appropriate for further analysis. However, the hardness value obtained in the current study cannot be in correlation with adhesion/cohesion strength due to the occurrence of microcracking on imprint and the dominance of substrate effect (shown in Fig. 10). Although it is difficult to measure the coating material bond strength directly by hardness, the adhesive/cohesive bond strength can be reflected by the comparison of critical applied load in scratch test and corresponding CoF between the sample with and without PVD sputtering. The corresponding CoF with respect to critical load applied in scratch test for all samples is shown in Table 3. When the applied load is 10 N, the corresponding CoF of all PVD sputtered samples is significantly lower than that of cold sprayed samples, indicating that the adhesive/cohesive strength of PVD sputtered coating under such load is sufficiently strong, PVD coatings (i.e. PVD Ti–6Al and PVD Ti–10Al) still adhere to the cold sprayed subsurface. This also implies that the coating material (i.e. PTFE + Al_2O_3) has a higher resistance to contact deformation and better deformability under this applied load. When the load exceeds 20 N, the corresponding CoF of all PVD sputtered samples shows a similar value to that of cold sprayed samples, clearly revealing that the coating material cannot withstand such high load and cause damage to coating system with substrate exposure. Therefore, it can be concluded that the order of adhesion/cohesion strength of PVD sputtered coating is: PVD Ti–6Al > CPVD Ti–6Al > CPVD Ti–10Al ≥ PVD Ti–10Al > PVD Ti–50Al ≈ CPVD Ti–50Al.

3.4. *Coating resistance to rockwell indentations*

The coating resistance to load indentation was assessed by the Rockwell indentation method. The corresponding applied stress and the circumferential indentation patterns (shown in Fig. 10) were reviewed on the sample of PVD magnetron sputtered Ti–6Al. The average indentation diameter for the applied load of 10 N is approximately 123.7 ± 7.6 µm. The radius of the indentation mark is the depth of the indentation tested by Rockwell, for example about 61.9 µm, which is greater than the thickness of the PVD sputtered thin film. Therefore, the Rockwell hardness value does not truly represent the hardness of

PVD sputtered thin film (PTFE + Al_2O_3) due to the dominance of substrate effect (e.g. hardness value mostly expresses the hardness of cold sprayed Ti–6Al). However, the indentation morphology and the calculated applied stress of the different applied loads by the Rockwell hardness test are still very useful and a supplementary result of the scratch test [36]. For an applied load of 10 N, the indentation mark on PVD sputtered sample is well identified without any notable coating failure, cracks or delamination. This indicates that the coating system (PVD sputtered PTFE + Al_2O_3 and cold sprayed Ti–6Al) is remains coherent under an applied load of 10 N, which corroborates the results observed in the scratch test (shown in Fig. 5). In addition, the contact pressure of acetabular for free speed unaided gait is reported around 4–6 MPa [37]. Therefore, this coating system offers protection of artificial joint surfaces as the corresponding applied stress to this coating by the Rockwell test is approximately 832.1 MPa (i.e. applied load: 10 N), which is much greater than the reported contact pressure of acetabular, and the coating can be assumed performing very well in the range of hydrodynamic lubrication regime without any coating failure. For loads up to 20 N in the Rockwell test, the coating system showed the onset of inter-particle de-bonding and micro-crack initiation around the indentation mark, suggesting that the coating system tends to lose effectiveness under these loads, and supported by the results obtained in the scratch test. Increasing the applied load to 30 N, the diameter of the resulting indentation mark increased to around 235 μm (assume the indentation depth is around 117 μm). As the thickness of the PVD sputtered thin film is only about 2% of the indentation depth, this implies that the self-lubricating effect of PVD sputtered film could be totally eliminated and the cold sprayed subsurface could be completely exposed under the stress of 30 N. This higher applied load is also associated with plastic deformation of the coating system and gives rise to severe wear, indicating that the mechanism of surface wear failure predominantly occurs under such applied load, and the results would play an important role in the application of this coating system in different working environments. As a result, both Rockwell indentation test and scratch test results are compatible, revealing that the PVD sputtered self-lubricating thin film, either in layer-by-layer approach or co-sputtered route are providing excellent frictional improvement below 10 N and are losing effectiveness above 20 N.

4. Conclusions

Metal matrix composite (MMC) coatings with various amount of Al content was initially fabricated by cold spray (CS) technology. Subsequently, PVD magnetron sputtering was then employed to prepare a self-lubricating thin film on top of MMC coatings, developing a robust damage tolerant coating system which can be used as a protective coating for existing movable artificial joints. The coating system was evaluated by SEM and EDX analysis, subsequently, the tribological properties of the self-lubricating coating were examined under scratch performance. The main conclusions are exhibited as follows:

1. Coatings inspection by SEM and EDX analysis indicated that PTFE + Al_2O_3 was successfully deposited on the MMC subsurface, forming a PTFE–Al_2O_3 nanocomposite in the case of the layer-by-layer approach.
2. The self-lubricating nature of the PTFE + Al_2O_3 thin film had remarkable effects on the reduction of the coefficient of friction (CoF) and mitigated the surface wear against a Rockwell diamond ball counter-part for MMC coatings.
3. Four critical regions were well identified from the graph of the CoF against continuous progressive load, indicating that a specific wear mechanism was found for the PVD sputtered PTFE + Al_2O_3 thin film.
4. Regardless of whether the PVD sputtered thin film was manufactured by a layer-by-layer approach or co-sputtering method, it demonstrated a superior frictional performance up to an applied force of 10 N, especially for the sample of cold sprayed Ti–6Al.
5. Prior to the applied force of 20 N, the coating system still provided self-lubricating effect, in particular, the PVD sputtered Ti–6Al and Ti–10Al were mainly carried out under a lubricious regime.
6. Above an applied force of 30 N, the self-lubricating effect provided by PTFE + Al_2O_3 thin film was eliminated, resulting in severe wear and crack initiation, and the MMC subsurface was exposed.
7. The reported contact pressure (i.e. around 4–6 MPa) of acetabular was far lower than the corresponding applied stress (i.e. applied load: 10 N; corresponding applied stress: 832.1 MPa) to the coating system by the Rockwell test, recommending that this coating system is ideal for protecting the surface of artificial joints.

Conflict of interest

The authors declare no conflicts of interest.

Acknowledgements

The authors would like to thank Dr Rocco Lupoi and Dr Shuo Yin for the support in developing the coating system. The work was financially supported by Surface Engineering and Precision Institute (SEPi) at Cranfield University. The work was also partly supported by the visiting research studentship provided by Department of Mechanical and Manufacturing Engineering, Trinity College Dublin, The University of Dublin, Dublin, Ireland.

REFERENCES

[1] Apostu D, Lucaciu O, Berce C, Lucaciu D, Cosma D. Current methods of preventing aseptic loosening and improving osseointegration of titanium implants in cementless total hip arthroplasty: a review. J Int Med Res 2018;46(6):2104–19.
[2] Ng CH. Investigation of damage tolerance coating system for biomedical. Cranfield, U.K.: Cranfield University; 2018.
[3] Harris KL, Pitenis AA, Sawyer WG, Krick BA, Blackman GS, Kasprzak DJ, et al. PTFE tribology and the role of mechanochemistry in the development of protective surface films. Macromolecules 2015;48(11):3739–45.

[4] Breki A, Nosonovsky M. Ultraslow frictional sliding and the stick–slip transition. Appl Phys Lett 2018;113(24):241602.
[5] Dhanumalayan E, Joshi GM. Performance properties and applications of polytetrafluoroethylene (PTFE) – a review. Adv Compos Hybrid Mater 2018;1(2):247–68.
[6] Teo AJ, Mishra A, Park I, Kim YJ, Park WT, Yoon YJ. Polymeric biomaterials for medical implants and devices. ACS Biomater Sci Eng 2016;2(4):454–72.
[7] Catanese J III, Cooke D, Maas C, Pruitt L. Mechanical properties of medical grade expanded polytetrafluoroethylene: the effects of internodal distance, density, and displacement rate. J Biomed Mater Res 1999;48(2):187–92.
[8] Mori H, Gupta A, Torii S, Harari E, Jinnouchi H, Virmani R, et al. Clinical implications of blood–material interaction and drug eluting stent polymers in review. Expert Rev Med Dev 2017;14(9):707–16.
[9] Zhou Y, Tan J, Dai Y, Yu Y, Zhang Q, Meyerhoff ME. Synthesis and nitric oxide releasing properties of novel fluoro S-nitrosothiols. Chem Commun 2019;55(3):401–4.
[10] Beckford S, Zou M. Wear resistant PTFE thin film enabled by a polydopamine adhesive layer. Appl Surf Sci 2014;292:350–65.
[11] Shen JT, Top M, Pei YT, De Hosson JTM. Wear and friction performance of PTFE filled epoxy composites with a high concentration of SiO_2 particles. Wear 2015;322:171–80.
[12] Sieh R, Le H. Non-cyanide electrodeposited Ag–PTFE composite coating using direct or pulsed current deposition. Coatings 2016;6(3):31.
[13] Haneef M, Rahman JF, Yunus M, Zameer S, Patil S, Yezdani T. Hybrid polymer matrix composites for biomedical applications. Int J Mod Eng Res 2013;3:970–9.
[14] Kamegawa T, Shimizu Y, Yamashita H. Superhydrophobic surfaces with photocatalytic self-cleaning properties by nanocomposite coating of TiO_2 and polytetrafluoroethylene. Adv Mater 2012;24(27):3697–700.
[15] Sawyer WG, Freudenberg KD, Bhimaraj P, Schadler LS. A study on the friction and wear behavior of PTFE filled with alumina nanoparticles. Wear 2003;254(5–6):573–80.
[16] Burris DL, Sawyer WG. Improved wear resistance in alumina-PTFE nanocomposites with irregular shaped nanoparticles. Wear 2006;260(7–8):915–8.
[17] Burris DL, Sawyer WG. Tribological sensitivity of PTFE/alumina nanocomposites to a range of traditional surface finishes. Tribol Trans 2005;48(2):147–53.
[18] Anjum SS, Rao J, Nicholls JR. Polymer (PTFE) and shape memory alloy (NiTi) intercalated nano-biocomposites. IOP Conf Ser: Mater Sci Eng 2012;40(1):012006.
[19] Rao J, Anjum SS, Craig M, Nicholls JR. Bioinspired metal–polymer thin films with varying hydrophobic properties. J Coat Technol Res 2018;15(1):87–94.
[20] Cavaleiro AJ, Ramos AS, Martins RMS, Fernandes FB, Vieira MT. The effect of heating rate on the phase transformation of Ni/Ti multilayer thin films. Vacuum 2017;139:23–5.
[21] Amirzada MR, Tatzel A, Viereck V, Hillmer H. Surface roughness analysis of SiO_2 for PECVD, PVD and IBD on different substrates. Appl Nanosci 2016;6(2):215–22.
[22] Wang Z, Wu L, Qi Y, Cai W, Jiang Z. Self-lubricating Al_2O_3/PTFE composite coating formation on surface of aluminium alloy. Surf Coat Technol 2010;204(20):3315–8.
[23] Biederman H. RF sputtering of polymers and its potential application. Vacuum 2000;59(2–3):594–9.
[24] Schürmann U, Hartung W, Takele H, Zaporojtchenko V, Faupel F. Controlled syntheses of Ag–polytetrafluoroethylene nanocomposite thin films by co-sputtering from two magnetron sources. Nanotechnology 2005;16(8):1078.
[25] Biederman H, Zeuner M, Zalman J, Bílkoá P, Slavínská D, Stelmasuk V, et al. Rf magnetron sputtering of polytetrafluoroethylene under various conditions. Thin Solid Films 2001;392(2):208–13.
[26] Carreri FC, Bandorf R, Gerdes H, Vergöhl M, Bräuer G. Highly insulating alumina films by a bipolar reactive MF sputtering process with special arc handling. Surf Coat Technol 2016;290:82–6.
[27] Tang X, Li Z, Liao H, Zhang J. Growth of ultrathin Al_2O_3 films on n-InP substrates as insulating layers by RF magnetron sputtering and study on the optical and dielectric properties. Coatings 2019;9(5):341.
[28] Segda BG, Jacquet M, Besse JP. Elaboration, characterization and dielectric properties study of amorphous alumina thin films deposited by r.f. magnetron sputtering. Vacuum 2001;62(1):27–38.
[29] Hanby BV, Stuart BW, Gimeno-Fabra M, Moffat J, Gerada C, Grant DM. Layered Al_2O_3–SiO_2 and Al_2O_3–Ta_2O_5 thin-film composites for high dielectric strength, deposited by pulsed direct current and radio frequency magnetron sputtering. Thin Solid Films 2018;662:145–54.
[30] Tang A, Wang M, Huang W, Wang X. Composition design of Ni–nano-Al_2O_3–PTFE coatings and their tribological characteristics. Surf Coat Technol 2015;282:121–8.
[31] Ye J, Burris DL, Xie T. A review of transfer films and their role in ultra-low-wear sliding of polymers. Lubricants 2016;4(1):4.
[32] Uruena JM, Pitenis AA, Harris KL, Sawyer WG. Evolution and wear of fluoropolymer transfer films. Tribol Lett 2015;57(1):9.
[33] Pitenis AA, Harris KL, Junk CP, Blackman GS, Sawyer WG, Krick BA. Ultralow wear PTFE and alumina composites: it is all about tribochemistry. Tribol Lett 2015;57(1):4.
[34] Green AP. Friction between unlubricated metals: a theoretical analysis of the junction model. Proc R Soc Lond Ser A. Math Phys Sci 1955;228(1173):191–204.
[35] Kusakabe S, Rawls HR, Hotta M. Relationship between thin-film bond strength as measured by a scratch test, and indentation hardness for bonding agents. Dent Mater 2016;32(3):e55–62.
[36] Zhang P, Li SX, Zhang ZF. General relationship between strength and hardness. Mater Sci Eng A 2011;529:62–73.
[37] Krebs DE, Robbins CE, Lavine L, Mann RW. Hip biomechanics during gait. J Orthop Sports Phys Ther 1998;28(1):51–9.

Cranfield University

CERES Research Repository **https://dspace.lib.cranfield.ac.uk/**

School of Aerospace, Transport and Manufacturing (SATM) Staff publications (SATM)

The role of PVD sputtered PTFE and Al2O3 thin films in the development of damage tolerant coating systems

Ng, Chi-Ho

2019-12-09

Attribution-NonCommercial-NoDerivatives 4.0 International

Ng CH, Rao J, Nicholls J. (2019) The role of PVD sputtered PTFE and Al2O3 thin films in the development of damage tolerant coating systems. Journal of Materials Research and Technology, Volume 9, Issue 1, January–February 2020, pp. 675-686

https://doi.org/10.1016/j.jmrt.2019.11.009

Downloaded from CERES Research Repository, Cranfield University